Pergamon

Geochimica et Cosmochimica Acta, Vol. 66, No. 5, pp. 829–836, 2002

0016-7037/02 $22.00 + .00

PII S0016-7037(02)00805-5

Surface chemistry and structural properties of mackinawite prepared by reaction of sulfide ions with metallic iron

MARTINE MULLET,* SOPHIE BOURSIQUOT, MUSTAPHA ABDELMOULA, JEAN-MARIE GÉNIN, and JEAN-JACQUES EHRHARDT

[1]Laboratoire de Chimie Physique et Microbiologie pour l'Environnement, UMR 7564 CNRS-Université Henri Poincaré-Nancy 1, 405, rue de Vandœuvre, F-54600 Villers-lès-Nancy, France

(*Received December* 22, 2000; *accepted in revised form August* 17, 2001)

Abstract—Tetragonal FeS_{1-x} mackinawite, has been synthesized by reacting metallic iron with a sodium sulfide solution and characterized by X-ray diffraction (XRD), transmission electron microscopy (TEM), transmission Mössbauer spectroscopy (TMS) and X-ray photoelectron spectroscopy (XPS). Based on XRD and TEM analyses, synthetic mackinawite exhibits crystallization and is identical to the natural mineral. Unit cell parameters derived from XRD data are $a = b = 0.3670$ nm and $c = 0.5049$ nm. The bulk Fe:S ratio derived from the quantitative dispersive energy analysis is practically 1. XPS analyses, however, showed that mackinawite surface is composed of both Fe(II) and Fe(III) species bound to monosulfide. Accordingly, monosulfide is the dominant S species observed at the surface with lesser amount of polysulfides and elemental sulfur. TMS analysis revealed the presence of both Fe(II) and Fe(III) in the mackinawite structure, thus supporting the XPS analysis. We propose that the iron monosulfide phase synthesized by reacting metallic iron and dissolved sulfide is composed of Fe(II) and S(-II) atoms with the presence of a weathered thin layer covering the bulk material that consists of both Fe(II) and Fe(III) bound to S(-II) atoms and in a less extent of polysulfide and elemental sulfur. *Copyright © 2002 Elsevier Science Ltd*

1. INTRODUCTION

Mackinawite, a tetragonal sulfur-deficient iron (II) sulfide of composition FeS_{1-x} with $0 < x < 0.07$ (Vaughan and Craig, 1978) is an important earth mineral. First, it can contain significant amounts of Ni, Co and Cu, and is known as a major ore mineral for Ni and Co. Secondly, mackinawite may entrap heavy pollutant metals like Cr and As, thus playing an important role in the remediation of contaminated sites (Patterson et al., 1997; Holmes, 1999). Finally, the discovery of life forms adapted to the warm anoxic environments of sea-floor hydrothermal systems, and the known sulfur-metabolizing ancient bacteria, has suggested that the emergence of life on earth could have occurred from anoxic iron sulfide environments.

At low temperatures, the most common phases of the Fe-S systems are "amorphous FeS" that transforms on ageing into mackinawite, greigite (Fe_3S_4), pyrrhotite ($Fe_{1-x}S$), marcasite (FeS_2, orthorombic), pyrite (FeS_2, cubic) and troilite (FeS). The importance of mackinawite lies mainly in its role as a precursor to the formation of most other iron sulfide phases (Rickard, 1969a; Sweeney and Kaplan, 1973), among which pyrite (FeS_2) is the most abundant. Finally, the experimental conditions under which the formation of a specific iron sulfide phase in the Fe-S system is favoured are well summarized by Lennie and Vaughan (1996).

The formation of mackinawite takes place in recent sediments (Berner, 1967) via sulphate-reducing bacteria, and in presently active hydrothermal systems or near midocean ridges (Vaughan and Craig, 1978). The biologic process is the result of the oxidation of organic matter that occurs through bacterial reduction of sulphate correlative to the production of hydrogen sulfide. Hydrogen sulfide then reacts with iron species from detritus or other sources to form an amorphous precipitate which, within days, crystallizes to the more stable mackinawite. A direct precipitation mechanism between iron and sulfide species is also encountered in hydrothermal sulfide deposits associated with volcanic activity.

The mackinawite structure of P4/nmm space group consists of a distorded cubic-packed array of sulfur atoms with iron in some of the tetrahedral interstices but vacancies in the larger octahedral spaces (Taylor and Finger, 1970). Iron atoms are at the centre of slightly distorted tetrahedra sharing edges to form sheets (Fig. 1). These are stacked along the *c* axis, with only weak Van der Waals forces holding them together. Moreover, mackinawite is able to accommodate cations in excess in the large octahedral vacancies of the structure (Vaughan, 1970), thus explaining why natural mackinawite appears commonly with significant amounts of metals other than iron (Vaughan, 1970; Mukherjee and Sen, 1991).

Two major ways for synthesizing mackinawite are encountered in the literature; they involve either the precipitation of aqueous Fe(II) (Rickard, 1969a; Patterson et al. 1997) or the reaction of metallic iron (Berner, 1964, Lennie et al., 1995) with a dissolved sulfide solution. Electrochemical synthesis under an applied potential has also been reported (Yamaguchi and Moori, 1972; Bezdicka et al., 1989). Dry synthesis is less usual (Takeno et al., 1982) where dry iron sulfide melts with contents of either Co and/or Ni or Cu were heated to high temperatures and chilled; re-equilibration of the products at different temperatures then resulted in the mackinawite formation.

Up till now, most information reported in the literature concerns the more thermodynamically stable iron sulfide phases such as pyrrhotite and pyrite. In fact, mackinawite is very reactive toward oxygen and important efforts must be made to avoid oxidation making it difficult to characterize.

* Author to whom correspondence should be addressed (mullet@lcpe.cnrs-nancy.fr).

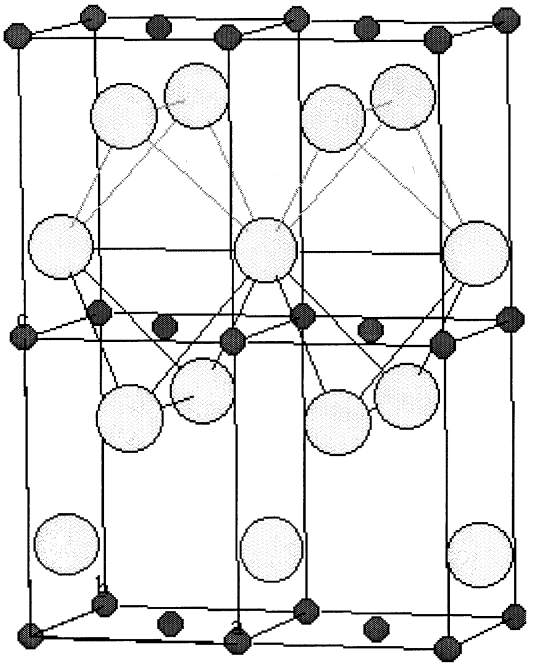

Fig. 1. Mackinawite structure. Small and large spheres represent Fe and S atoms respectively.

Therefore, there are either a lack of information or discrepancies reported in the literature that concern the surface and bulk oxidation states as well as the magnetic and structural properties of mackinawite (Morice et al., 1969; Vaughan and Ridout, 1971; Herbert et al., 1998). However, the knowledge of these data is of utmost importance in assessing the mackinawite reactivity and in particular its ability to transform to more stable phases like pyrite. In this study, mackinawite was synthesized from metallic iron and an aqueous sulfide solution and characterized by using X-ray diffraction (XRD), transmission electron microscopy (TEM), transmission Mössbauer spectroscopy (TMS) and X-ray photoelectron spectroscopy (XPS). The data yielded new information concerning the oxidation state and structural properties of synthetic mackinawite. They also may help for understanding the formation of the more stable phase greigite from the mackinawite structure.

2. MATERIAL AND METHODS

2.1. Mackinawite Synthesis

The reactivity of mackinawite with oxygen required great care for preventing its oxidation during synthesis and subsequent handling. All reagents were thus prepared using deionised distilled water (ca 18 $M\Omega^{-1}$) that had been purged by bubbling nitrogen during thirty minutes. Moreover, the mackinawite synthesis and the preparation of samples for analyses were conducted in a nitrogen-purged Jacomex® controlled atmosphere glovebox.

Mackinawite was synthesized according to the method described by Lennie et al. (1995). An iron wire of 5 g was immersed in 500 cm^3 of a 0.5M acetic acid/acetate buffer (pH = 4.6). Partial dissolution of the iron wire by reaction with the acetate buffer (~3.5 h) evolved H_2 gas and provided a reducing environment. 30 cm^3 of a 0.45M Na_2S solution was then slowly added to the reaction vessel and black particles immediately precipitated. This solution was allowed to stand open for 24 h. The remnant iron wire was then removed and the supernatant discarded. The formed mackinawite was washed and filtered several times with de-aerated and de-ionised water before being freeze-dried. To limit the storage time of mackinawite samples, analyses were performed immediately after synthesis.

2.2. Instrumentation

2.2.1. X-ray diffraction analysis (XRD)

X-ray powder diffraction patterns were obtained from a classical powder diffractometer with transmission geometry, equipped with a Mo tube ($K\alpha_1$ radiation, λ=0.070930 nm), a quartz monochromator and a scintillation counter. Mackinawite powder was poured into a Lindemann glass tube (1mm diameter and 0.01 mm thick), that was sealed immediately. The mackinawite sample was step-scanned from 2 to 40°(2θ) using a step of 0.05°(θ). The angular resolution was 0.04°. However it was increased up to 0.08° due to the thickness of the Lindemann glass.

2.2.2. Transmission electron microscopy (TEM)

A Philips® CM20 transmission electron microscope operating at 120 keV and equipped with an energy dispersive spectrometer was used to examine the synthetic mackinawite sample. A suspension of mackinawite prepared in ethanol was quickly dispersed in the air onto an amorphous carbon-coated grid and loaded into the analysis holder of the microscope. Identification of mackinawite was made from both selected-area diffraction patterns and energy-dispersive analysis.

2.2.3. Transmission mössbauer spectroscopy (TMS)

The Mössbauer spectra by transmission (TMS) were obtained by use of a constant acceleration Mössbauer spectrometer with a 50 mCi source of ^{57}Co in Rh. The spectrometer was calibrated with a 25 μm foil of α-Fe at room temperature and the isomer shifts δ are relative to this reference. The cryostat consisted of a closed-cycle helium Mössbauer cryogenic workstation with vibrations insulation stand manufactured by Cryo Industries of America®. Helium exchange gas was used to thermally couple the sample to the refrigerator, allowing variable temperature operation from 11 to 300 K. Computer fittings were done using Lorentzian-shape lines. The parameters that result from any computer fitting must be both mathematically (χ^2 minimisation) and physically significant; in particular the width of all lines must be small enough. The samples were prepared for TMS measurements in a nitrogen atmosphere in the glovebox and quickly transferred to the sample holder in a cryostat at room or low temperatures in an inert He atmosphere.

2.2.4. X-ray photoelectron spectroscopy (XPS)

X-ray photoelectron spectra were obtained with a VSW HA150 MCD® electron energy analyser using a Mg$K\alpha$ non-

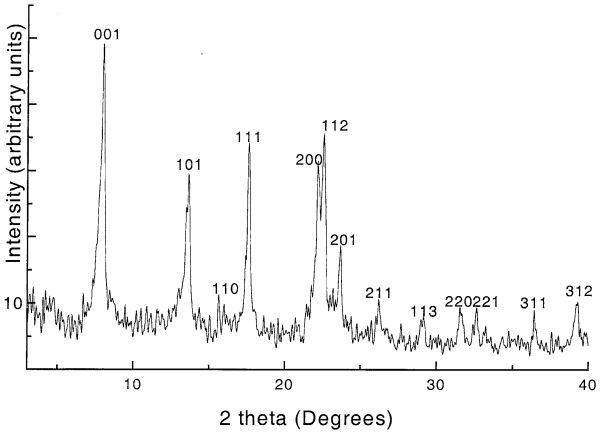

Fig. 2. X-ray diffraction pattern for synthetic mackinawite (MoKα_1, $\lambda = 0.070930$ nm).

monochromatic source (1253.6 eV). Energy resolution was 0.8 eV. The base pressure in the analytical chamber was of the order of 10^{-9} mbar. The energy scale was calibrated using the Au($4f_{7/2}$) (84.0 eV) and Ag($3d_{5/2}$) (368.2 eV) lines. Survey and narrow XPS spectra were obtained with an analyser pass energy of 90 and 22 eV, respectively. Raw spectra were smoothed before being fitted using a Shirley base line and a Gaussian-Lorentzian shape peak. The aliphatic adventitious hydrocarbon C(1s) peak at 284.6 eV was adopted as a check for surface charging. The mackinawite sample was pressed on a copper tape in the glovebox and quickly transferred to the XPS spectrometer under a continuous nitrogen flow. Narrow scanned spectra were used to obtain the chemical state information for iron (Kinetic energy $E_k \sim 546$ eV), sulfur ($E_k \sim 1093$ eV) and oxygen ($E_k \sim 724$ eV). The inelastic mean free paths derived from the kinetic energies are in the range $\lambda_{IMFP} \sim 10$ to 20 Å.

3. RESULTS

3.1. X-ray Diffraction Analysis (XRD)

The initial identification of synthetic mackinawite was performed using XRD. The lines of the diffraction pattern, presented in Figure 2, are indicative of a crystalline phase, with line intensities and positions in good agreement with previously reported data for mackinawite (Rickard, 1969a). Unit cell parameters derived from the diffraction pattern of Figure 2 are $a = b = 0.367$ nm and $c = 0.505$ nm. Lennie et al. (1997) observed additional reflections due to α-Fe remaining from synthesis.

3.2. Transmission Electron Microscopy (TEM)

The synthetic mackinawite was further characterized using TEM. The examination of mackinawite particles (Fig. 3) shows irregular shape single crystals of approximately 1 to 2 μm; these particles appeared often in aggregates on the carbon grid. The quantitative dispersive energy analysis, performed on several individual particles, indicated only the presence of Fe and S with an average S:Fe atomic ratio of 0.99 and an estimated standard deviation of 0.08. This mackinawite composition agrees with that reported in the literature, that is FeS_{1-x} with

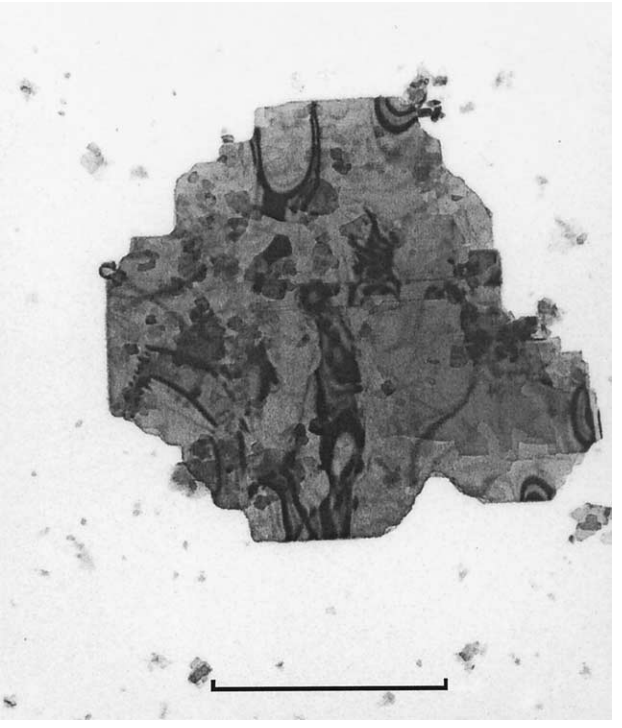

Fig. 3. TEM image of a mackinawite particle (the scale bar is 1 μm).

$0 < x < 0.07$ (Vaughan and Craig, 1978). Single crystals showed characteristic electron diffraction patterns consistent with mackinawite crystals lying with (001) plane parallel to the carbon grid. One example of this pattern is shown in Figure 4. No other phases were observed in TEM experiments.

3.3. Transmission Mössbauer Spectroscopy (TMS)

Transmission Mössbauer spectroscopy was used to investigate the oxidation states, structural and magnetic properties of synthetic mackinawite. Until now, few TMS data have been available for this mineral and no general agreement exists between various authors. According to Morice et al. (1969), the Mössbauer spectrum of synthetic mackinawite at room temperature is rather complex, having at least three sextets. In contrast, Vaughan and Ridout (1971) obtained one singlet, even down to 4 K (Table 1) and magnetic lines of relatively low intensity on either side of the singlet, attributed to remaining iron and greigite impurities. The Mössbauer spectrum of synthetic mackinawite obtained in the present study at room temperature over a wide velocity range ($\pm$ 11 mm s^{-1}) is presented in Figure 5a. Although it shows good agreement with those of Vaughan and Ridout (1971), the Mössbauer spectrum presented here cannot be fitted as only one singlet that results from low spin Fe(II) in tetrahedral sites since the line looks asymmetrical. The fitting of the Mössbauer spectrum over a smaller velocity range ($\pm$ 3 mm s^{-1}) can reasonably be described as a superimposition of elemental subspectra: one singlet S_1 and two doublets D_1 and D_2 as shown in Figure 5b. Corresponding hyperfine parameters are given in Table 2. According to the structure of mackinawite derived from both XRD and TEM

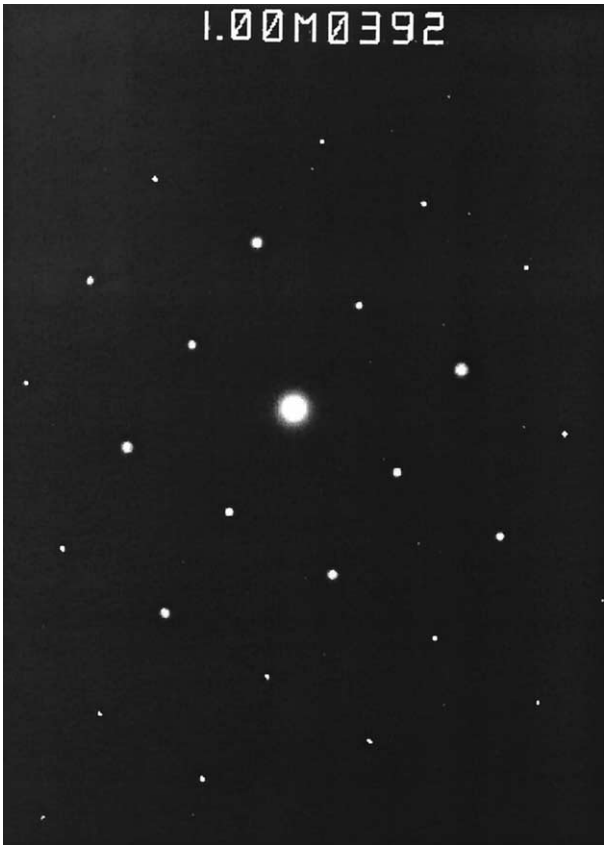

Fig. 4. Electron diffraction pattern obtained along [001] zone axis.

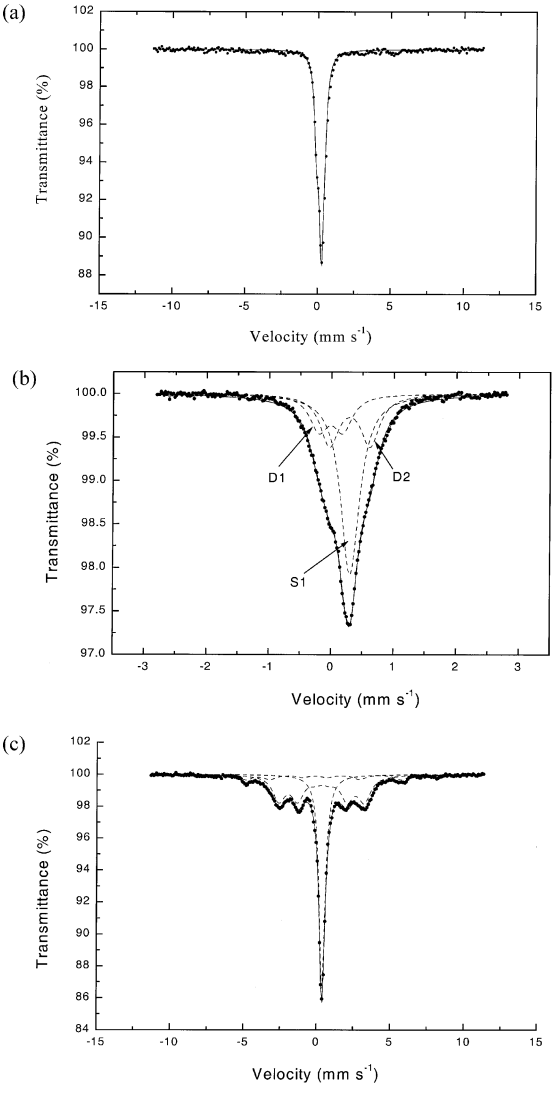

Fig. 5. a. Mössbauer spectrum measured at room temperature of synthetic mackinawite on a wide velocity range. Circles are experimental data and solid line is the fitted curve. Figure 5b. Mössbauer spectrum measured at room temperature of synthetic mackinawite. δ, isomer shift relative to metallic iron. Circles are experimental data; dashed lines are elementary components and solid line is the fitted curve. Figure 5c. Mössbauer spectrum at 11 K of synthetic mackinawite. Circles are experimental data; dashed lines are elementary components and solid line is the fitted curve.

experiments, iron cations are only located in tetrahedral sites. Thus, singlet S_1, characterized by an isomer shift δ of ~0.4 mm s^{-1}, corresponds to low spin Fe(II) in common tetrahedral sites (Vaughan and Ridout, 1971). However, S_1 represents only 52% of the whole area of the spectrum and two quadrupole doublets D_1 and D_2 are superimposed to it with respective relative abundance of 19 and 29%. The isomer shift δ of the first doublet D_1 is different from that of the singlet S_1, thus characterizing iron atoms in a different oxidation state. Its δ value likely characterizes low spin Fe(III). The discrimination between octahedral and tetrahedral sites from quadrupole splitting Δ is known to be very complex for low spin compounds like mackinawite. Besides, Fe(III) could be located both in tetrahedral sites in substitution of Fe(II) atoms and in large octahedral vacancies in the structure. Although it is not possible to definitely eliminate one of these two assumptions, only tetrahedral coordination of Fe by S has been observed in EXAFS spectra of mackinawite synthesized from metallic iron and sulfide solution (Lennie and Vaughan, 1996). The second doublet D_2, which has the same isomer shift as singlet S_1, characterizes also a low spin Fe(II) but its Δ value of 0.6 mm s^{-1} indicates a new environment which may be caused by the presence of an Fe(III) ion as next nearest neighbour. Thus, we interpret singlet S_1 as low spin Fe(II) atoms in tetrahedral sites with no Fe(III) as nearest neighbour, found in bulk mackinawite, doublet D_1 as Fe(III) atoms likely in tetrahedral sites and doublet D_2 as Fe(II) atoms in tetrahedral sites close to an Fe(III) ion. About 80% of the whole relative abundance in the Mössbauer spectrum correspond to Fe(II) atoms in tetrahedral sites and ~20% to Fe(III) ions if Lamb-Mössbauer factors f are assumed to be equal.

The Mössbauer spectrum of synthetic mackinawite at 11 K (Fig. 5c) shows that the sample orders magnetically by lowering the temperature. An acceptable fit to the data is obtained with one singlet and two sextets. The δ value of singlet S_1 at 11 K is increased to 0.53 mm s^{-1} by second order Doppler shift. The presence of the singlet at low temperature agrees with the literature data reported by Bertaut (1965) and Vaughan and Ridout (1971) and is still attributed to Fe(II) ions in tetrahedral sites of bulk mackinawite. The two sextets are discriminated by their values of hyperfine field, 181 and 329 kOe, and could be interpreted as iron (II) and iron (III) in agreement with the

Table 1. Mössbauer parameters reported in the literature for synthetic mackinawite.

References	T[a] (K)	δ[b] (mm s^{-1})	ΔE_Q[c] (mm s^{-1})	H[d] (KOe)
Morice et al. (1969)	298	0.65 ± 0.04	0.09 ± 0.06	298 ± 5
		0.59 ± 0.04	0.06 ± 0.06	262 ± 5
		0.62 ± 0.04	0.09 ± 0.06	228 ± 5
Vaughan and Ridout (1971)	4.2	0.2	–	–

[a] T, Temperature.
[b] δ, Isomer shift relative to metallic iron.
[c] ΔE_Q, Quadrupole splitting.
[d] H, Hyperfine magnetic field.

interpretation of the Mössbauer data at room temperature. The hyperfine parameters of those sextets at 11 K deviate drastically from those of all iron oxides, which have magnetic hyperfine fields close to 500 kOe at 11 K.

3.4. X-ray Photoelectron Spectroscopy (XPS)

In contrast to TMS, which allows an analysis of the bulk material, XPS is only sensitive to the sample surface. The XPS survey scan of the synthetic mackinawite indicated the presence of O, C, S and Fe at the sample surface. Even by taking precautions during the synthesis and preparation of the sample for analysis, it was not possible to completely eliminate oxygen that adsorbed at the surface. Otherwise, carbon was a ubiquitous contaminant. The semiquantitative surface composition (±10%) was calculated from the peak areas (Fe(2p), S(2p) and O(1s)) and theoretical cross-sections (Scofield, 1976), which yielded approximately 19 (atomic) % O, 37% Fe and 44% S.

The narrow region spectra for Fe($2p_{3/2}$), S(2p) and O(1s) are shown in Figure 6. No charge correction was necessary. The broad Fe($2p_{3/2}$) spectrum (Fig. 6a) presents a major contribution occurring near 707 eV, which corresponds to the binding energy of Fe(II)-S compounds (Mycroft et al., 1990; Nesbitt et al., 1998, Lennie and Vaughan, 1996). The shape of this peak is very similar to that obtained by Pratt et al. (1994a) for fresh fractured pyrrhotite or by Herbert et al. (1998) for mackinawite synthesized in media containing sulphate-reducing bacteria. Fe($2p_{3/2}$) binding energies for various model compounds are listed in Table 3 and the binding energies for the fitted Fe($2p_{3/2}$) peaks in this study are listed in Table 4. Over the Fe(II)-S component in mackinawite at 707± 0.1 eV (Table 3), Fe(II) of bulk mackinawite has a low spin configuration due to sulfur atoms, (cf. TMS results and Vaughan and Ridout 1971), and contributes to only one peak (no multiplet splitting) to the Fe($2p_{3/2}$) spectrum as observed in other studies (Nesbitt and Muir, 1994, Mycroft et al., 1990). Gupta and Sen (1974, 1975) calculated multiplet pattern for free ions of various transition metals. According to these authors the number of unpaired electrons determines the number and intensity of the multiplet signals. As low spin Fe(II) in mackinawite has only paired electrons at the t_2 level, a narrow single peak in the Fe($2p_{3/2}$) spectrum consequently represents it. However, the Fe($2p_{3/2}$) spectrum was too large to be fitted with only one Fe(II)-S component. Following the approach of Pratt et al. (1994b) and Herbert et al. (1998), the high energy portion of the spectrum was fitted with a Fe(III)-S component, taking into account multiplet contributions predicted from crystal field theory (Gupta and Sen, 1974, 1975). Low spin Fe(III) in mackinawite has one unpaired electron at the t_2 level, which induces a multiplet structure. Thus, the Fe(III)-S contribution appears as one main peak at 708.5 ± 0.1 eV and three multiplet peaks, each separated by ~1 eV and with peak area ratio relative to the first ferric sulfide component equals to 0.68, 0.24, and 0.11 (Table 4); this multiplet fit was in agreement with Fe(III) multiplet splitting for pyrrhotite (Pratt et al., 1994a), for mackinawite (Herbert et al. 1998) and as calculated for the free Fe^{3+} ion (Gupta and Sen, 1975). Utilising only these Fe(II)-S and Fe(III)-S components to fit the Fe($2p_{3/2}$) spectrum does not achieve a good fit. Attempts to fit the data with a Fe(III)-O component proved to be unsuccessful, but a favourable fit is obtained with a Fe(II)-O component. Another contribution to the breadth of the Fe($2p_{3/2}$) spectrum (Fig. 6a) towards high binding energies may result from a Fe(II)-O environment; in fact, the Fe(II) surface may be partially coordinated by oxygen, after a brief contact with air but before oxidation occurs (Eggleston et al., 1996). Moreover, non-oxidatively Fe(II)-O sites may also result from the hydroxylation of the surface. The Fe($2p_{3/2}$) peak for Fe(II)-O is located near 709 eV (Thomas et al., 1998, McIntyre and Zetaruk, 1977). For comparison, the Fe(III)-O environments, resulting from oxidation, have higher binding energies i.e., ~711 to 712 eV (Thomas et al., 1998). Therefore, inclusion of the three contributions, Fe(II)-S, Fe(II)-O and Fe(III)-S provides a good fit to the Fe($2p_{3/2}$) XPS spectrum; the interpretation is adopted as the most reasonable and demonstrates the consistency between XPS and TMS.

Each species in the S(2p) spectrum (Fig. 6b) is fitted with doublets that characterize the spin-orbit splitting of the S($2p_{1/2}$) and S($2p_{3/2}$) peaks. To adequately fit the S(2p) spectrum, three doublets with $2p_{3/2}$ components at 161.3 ± 0.1eV, 163.2 ±0.1eV and 165.3 ± 0.1eV are required. The binding energy of the doublet at 161.3 ± 0.1eV, representing 80% of the total

Table 2. Mössbauer parameters for synthetic mackinawite at room temperature (this study).

Environment	δ[a] (mm s^{-1})	ΔE_Q[b] (mm s^{-1})	Relative abundance (%)	Assignment
S_1	0.42	–	52	LS[c] $[Fe^{2+}]^{tetra}$
D_1	0.13	0.38	19	LS[c] $[Fe^{3+}]^{tetra}$
D_2	0.41	0.64	29	LS[c] $[Fe^{2+}]^{tetra}$

[a] δ, Isomer shift relative to metallic iron.
[b] ΔE_Q, Quadrupole splitting.
[c] LS, Low Spin.

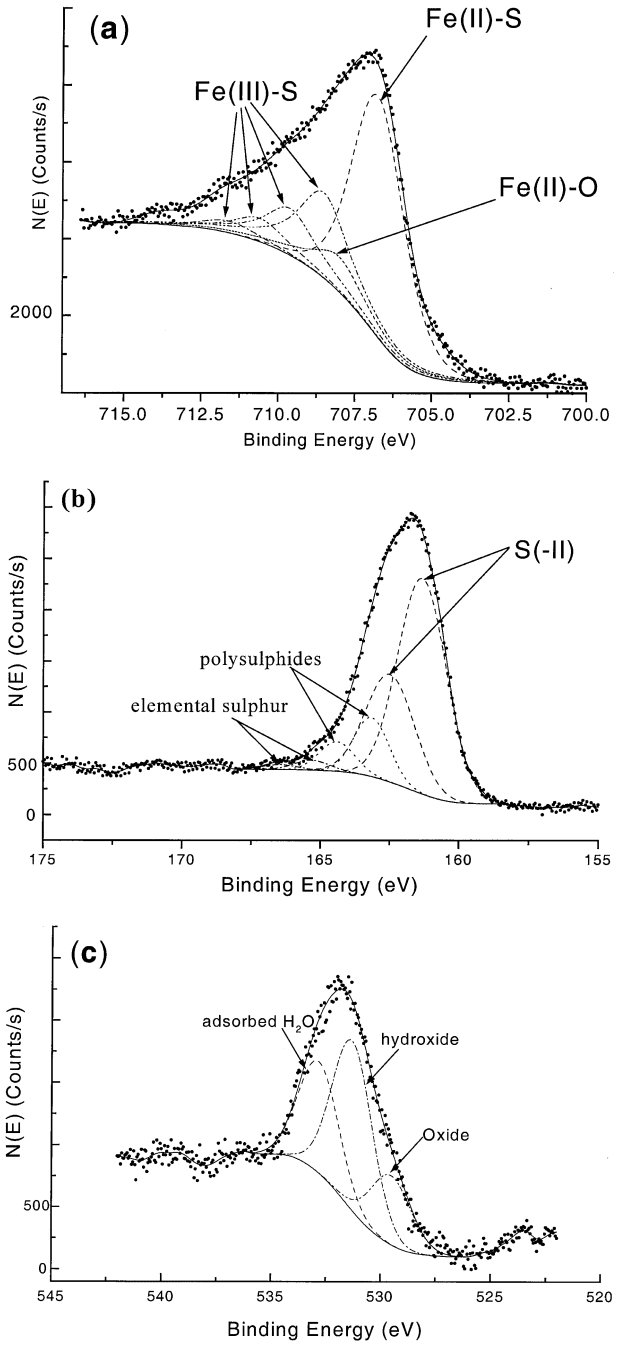

Fig. 6. Narrow scans of Fe(2p3/2), S(2p) and O(1s) XPS spectra (a to c respectively). Circles are experimental data; bottom solid line is the Shirley background; dashed lines are the fit to each spectrum and top solid line is the sum of background and fitted peaks.

S(2p) signal, is typically attributed to monosulfide species (Table 3); the second doublet is located at 163.2 eV ± 0.1eV and may correspond to polysulfides S_n^{2-} species (Table 3). The third doublet, which was fitted to take into account the high energy tail of the S(2p) spectrum is attributed to elemental sulfur S(0): the sum of these two last species is 20%. A low temperature measurement (liquid nitrogen) that was performed to limit the volatilisation of sulfur clearly confirmed the contribution of elemental sulfur and polysulfides to the S(2p) spectrum. These species reveal that some oxidation of the surface may have occurred (Benning et al. 2000, Taylor et al. 1979, Boursiquot et al. 2001).

Table 3. Binding energies for $Fe(2p_{3/2})$ S(2p) and O(1s) peaks in various model compounds in comparison with fitted peaks in Fig. 6.

Species	Binding energy (eV)	References
$Fe(2p_{3/2})$		
Fe(II)-S	707.0	Mycroft et al., 1990
	707.1	Pratt et al., 1994b
	707.3	Herbert et al., 1998
Fe(II)-O	709.5	McIntyre and Zetaruk, 1977
	709	Thomas et al., 1998
Fe(III)-S	709.2	Pratt et al., 1994b
	709.1	Herbert et al., 1998
	708.7	Nesbitt et al., 1998
Fe(III)-O	711.6	McIntyre and Zetaruk, 1977
	711	Thomas et al., 1998
	712	Thomas et al., 1998
	714	Thomas et al., 1998
	709.1/710.2/711.3/712.7	Pratt et al., 1997
$S(2p_{3/2})$		
S^{2-}	161.3	Pratt et al., 1994b
	160.9	Herbert et al., 1998
S_n^{2-}	163.3	Pratt et al., 1996
	163.4	Thomas et al., 1998
S°	164	Thomas et al., 1998
	164.4	Pratt et al., 1996
O(1s)		
O^{2-}	529.8	Jones et al., 1992
OH^-	531.4	McIntyre and Zetaruk, 1977
Adsorbed H_2O	532.6	Pratt et al., 1997

The O(1s) spectrum presented in Figure 6c is broad and is best fitted with three components at 529.5, 531.3 and 532.5 ± 0.1eV (Table 4). These correspond to oxide oxygen, hydroxyl groups and adsorbed water, respectively (Table 3). The oxide component supports the interpretation of the $Fe(2p_{3/2})$ spectrum with a Fe(II)-O contribution.

Table 4. Binding energies (BE), peak full width at half maximum (FWHM) and peak areas for $Fe(2p_{3/2})$, $S(2p_{3/2})$ and O(1s) photoelectron spectra (this study).

BE[a] (eV)	FWHM (eV)	Area (%)	Chemical species
$Fe(2p_{3/2})$			
706.8	2.0	47.7	Fe(II)-S
708	2.0	9.7	Fe(II)-O
708.5	2.0	21.9	Fe(III)-S
709.6	2.0	12.9	Fe(III)-S
710.6	2.0	5.4	Fe(III)-S
711.6	2.0	2.4	Fe(III)-S
$S(2p_{3/2})$[b]			
161.3	2.0	81.3	S^{2-}
163.2	1.5	16	S_n^{2-}
165.3	1.5	2.7	S°
O(1s)			
529.5	2.2	19.9	O^{2-}
531.3	2.2	48.4	OH^-
532.5	2.2	31.7	adsorbed H_2O

[a] Binding energy values are accurate to ± 0.1eV.
[b] Area for S(2p) spectrum includes $2p_{1/2}$ and $2p_{3/2}$ contributions.

4. DISCUSSION

Iron monosulfide (FeS) can be produced through the reaction between metallic or ferrous iron and aqueous sulfide solutions, at low temperatures (Rickard, 1969a; Berner, 1964; Lennie et al., 1995). The synthesis in media containing sulphate-reducing bacteria has been also reported (Rickard, 1969b). Some discrepancies appear in the XRD literature data relative to this precipitated iron monosulfide. It is reported as amorphous FeS (Patterson et al., 1997; Berner, 1964), poorly crystalline FeS with only the most intense X-ray line corresponding to the (001) plane (Rickard, 1995) and finally, as well crystallized mackinawite, that is with most X-ray lines developed (Rickard, 1969a; Lennie et al., 1995). In this study, both TEM and XRD results indicate that the major reaction product between metallic iron and an aqueous sulfide solution, in acidic conditions, is a crystalline phase. The X-ray diffraction analysis gives all the strongest characteristic lines of the natural mineral (Kouvo et al., 1963). The dependence of XRD pattern upon the method of preparation explains probably the different data reported in the literature. We tried to synthesize mackinawite from both metallic iron and ferrous iron, but it clearly appeared that the better-crystallized product was obtained using metallic iron, as already observed by Lennie and Vaughan (1996).

The S:Fe ratio derived from TEM experiments agrees with the bulk mackinawite composition reported in the literature, i.e., from $FeS_{0,93}$ to FeS (Vaughan and Craig, 1978). However, the semiquantitative surface composition calculated from the XPS survey scan yields to a S:Fe ratio of 1.2. Probably, elemental sulfur and polysulfide species detected in the XPS S(2p) spectrum explain this ratio. Moreover, the lack of a suitable background function for transition metal sulfides (McIntyre and Zetaruk, 1977; Pratt et al., 1994a) may also contribute to the overestimation of the S:Fe ratio. However, Berner (1964) and Rickard (1995) reported a S:Fe ratio of 1.1 for synthetic mackinawite suggesting the adsorption or coprecipitation of sulfide during synthesis.

The XPS results indicate the presence of Fe(II)-S and Fe(III)-S bond types at the mackinawite surface. The fit of the $Fe(2p_{3/2})$ XPS spectrum with a Fe(III)-O component appeared unlikely and the Fe(II)-O component is the result of oxygen adsorption that probably occurred during the transfer of the mackinawite sample from the glovebox to the XPS spectrometer vacuum chamber. The presence of both Fe(II) and Fe(III) coordinated with monosulfide at the surface of mackinawite (Herbert et al., 1998) as well as at the surface of other iron (II) sulfides like pyrite FeS_2 (Nesbitt and Muir, 1994) and pyrrhotite (Pratt et al., 1994a) has been previously discussed in the literature. In particular, Herbert et al. (1998) suggested that the mackinawite surface acquired a composition similar to greigite, the iron sulfide thiospinel Fe_3S_4 ($Fe_2^{(3+)}Fe^{(2+)}S_4^{(2-)}$). It was even claimed that the broadness of the $Fe(2p_{3/2})$ peak at the higher binding energy side of this peak could arise from the high conductivity in the (001) plane of mackinawite due to Fe-Fe interactions (Lennie and Vaughan, 1996).

The TMS analysis suggests the presence of both Fe(II) and Fe(III) in the mackinawite structure, thus supporting the XPS results. Mackinawite is a metastable iron sulfide, which transforms into sulfide phases like greigite and elemental sulfur (Posfai et al., 1998; Boursiquot et al. 2001) as well as iron (oxyhydr)oxide phases like goethite and magnetite (Benning et al. 2000; Boursiquot et al. 2001) in the presence of an oxidising agent (i.e., O_2, S(0). . .). Oxygen is not detected in the elemental analysis, despite the low sensitivity of this technique towards this light element, which is in agreement with the absence of a Fe(III)-O component in the $Fe(2p_{3/2})$ component. Consequently, the formation of iron oxides to explain the presence of Fe(III) in the mackinawite structure must be discarded.

Lennie et al. (1996) postulated that greigite is formed by the partial oxidation and rearrangement of some Fe(II) atoms within the cubic close packed sulfur array of mackinawite. The Fe(III) detected in the TMS experiments reveals the presence of a weathered layer encapsulating the bulk mackinawite crystals, which would consist of both Fe(II)-S and Fe(III)-S. This layer may be poorly ordered, thus explaining why it cannot be observed in diffraction experiments. The present study is not able to discriminate if this weathering layer is formed during synthesis or sampling. In particular, every operation that consists to separate the solid phase from the solution, i.e., vacuum drying or syringe filtering, may alter the properties of the surface (Morse and Arakaki, 1993, Herbert et al. 1998).

The whole results suggest that the iron monosulfide phase synthesized in the present study by reacting metallic iron and dissolved sulfide is composed of Fe(II) and S(-II) atoms with the presence of a weathered layer covering the mackinawite crystals that consists of both Fe(II) and Fe(III) bonded to S(-II) atoms and in a less extent of polysulfide and elemental sulfur. The presence of Fe(III)-S should be important to understand later the mackinawite-greigite transformation from mackinawite.

Acknowledgments—The authors wish to thank for assistance and helpful discussions: J. Lambert from 'Laboratoire de Chimie-Physique et Microbiologie pour l'Environnement, Villers-lès-Nancy, France', for XPS analysis, M. Lelaurain from 'Laboratoire de Chimie du Solide Minéral, Vandœuvre-les-Nancy, France' for XRD analyses. Dr J. Ghanbaja from the 'Service Commun de Microscopie Electronique par Transmission, Vandœuvre-les-Nancy, France' for TEM analyses.

Associate editor: S. J. Traina

REFERENCES

Benning L. G., Wilkin R. T., Barnes H. L. (2000) Reaction pathways in the Fe-S system below 100°C. *Chem. Geol.* **167,** 25–51.

Berner R. A. (1967) Thermodynamic stability of sedimentary iron sulfides. *Am. J. Sci.* **265,** 773–785.

Berner R. A. (1964) Iron sulfides formed from aqueous solutions at low temperatures and pressures. *J. Geol.* **72,** 293–306.

Bertaut E. F., Burlet P., Chappert J. (1965) Sur l'absence d'ordre magnétique dans la forme quadratique de FeS. *Solid State Commun.* **3,** 335–338.

Bezdicka P., Grenier J. C., Fournes L., Wattiaux A., Hagenmuller P. (1989) Electrochemical formation of mackinawite FeS: an in situ Mössbauer resonance study. *Eur. J. Sol. State Inor.* **26,** 353–365.

Boursiquot S., Mullet M., Abdelmoula M., Génin J. M., Ehrhardt J. J. (2001) The dry oxidation of mackinawite *Phys. Chem. Minerals* **28,** 600–611.

Eggleston C. M., Ehrhardt J. J., Stumm W. (1996) Surface structural controls on pyrite oxidation kinetics: an XPS-UPS, STM and modeling study. *Am. Mineral.* **81,** 1036–1056.

Gupta R. P., Sen S. K. (1974) Calculation of multiplet structure of core p-vacancy levels. *I. Phys. Rev. B.* **10,** 71–79.

Gupta R. P., Sen S. K. (1975) Calculation of multiplet structure of core p-vacancy levels. *II. Phys. Rev. B.* **12,** 15–19.

Herbert R. B. Jr, Benner S. G., Pratt A. R., Blowes D. W. (1998)

Surface chemistry and morphology of poorly crystalline iron sulfides precipitated in media containing sulfate-reducing bacteria. *Chem. Geol.* **144,** 87–97.

Holmes J. (1999) Fate of incorporated metals during mackinawite oxidation in sea water. *Appl. Geochim.* **14,** 277–281.

Jones C. F., Lecount S., Smart R. St. C., White T. (1992) Compositional and structural alteration of pyrrhotite surfaces in solution: XPS and XRD studies. *Appl. Surf. Sci.* **55,** 65–85.

Kouvo O., Vuorelainen Y., Long J. V. P. (1963) A tetragonal iron sulfide. *Am. Mineral.* **48,** 511–524.

Lennie A. R., Vaughan D. J. (1996) Spectroscopic studies of iron sulfide formation and phase relations at low temperatures. *Mineral Spectroscopy: A tribute to R.G. Burns.* **5,** 117–131.

Lennie A. R., Redfern S. A. T., Champness P. E., Stoddart C. P., Schofield P. F., Vaughan D. J. (1997) Transformation of mackinawite to greigite:an in situ X-ray powder diffraction and transmission electron microscopy study. *Am. Mineral.* **82,** 302–309.

Lennie A. R., Redfern S. A. T., Schofield P. F., Vaughan D. J. (1995) Synthesis and Rietveld crystal structure refinement of mackinawite, tetragonal FeS. *Mineral. Mag.* **59,** 577–683.

McIntyre N. S., Zetaruk D. G. (1977) X-ray photoelectron spectroscopic studies of iron oxides. *Anal. Chem.* **49,** 1521–1529.

Morice J. A., Rees L. V. C., Rickard D. T. (1969) Mössbauer studies of iron sulfides. *J. Inorg. Nucl. Chem.* **31,** 3797–3802.

Morse J. W., Arakaki T. (1993) Adsorption and coprecipitation of divalent metals with mackinawite (FeS). *Geochim. Cosmochim. Acta* **57,** 3635–3640.

Mukherjee A. D., Sen P. P. (1991) Compositional variations in mackinawites from the Chandmari mine of Ketri Copper Belt, Rajasthan. *J. Geol. Soc. India.* **38,** 96–100.

Mycroft J. R., Bancroft G. M., McIntyre N. S., Lorimer J. W., Hill I. R. (1990) Detection of sulfur and polysulfides on electrochemically oxidised pyrite surfaces by X-ray photoelectron spectroscopy and Raman spectroscopy. *J. Electroanal. Chem.* **292,** 139–152.

Nesbitt H. W., Muir I. J. (1994) X-ray photoelectron spectroscopic study of a pristine pyrite surface reacted with water vapour and air. *Geochim. Cosmochim. Acta.* **58,** 4667–4679.

Nesbitt H. W., Bancroft G. M., Pratt A. R., Scaini M. J. (1998) Sulfur and iron surface states on fractured pyrite surfaces. *Am. Mineral.* **83,** 1067–1076.

Patterson R. R., Fendorf S., Fendorf M. (1997) Reduction of hexavalent chromium by amorphous iron sulfide. *Env. Sci. Tech.* **31,** 2039–2044.

Posfai M., Buseck P. R., Bazylinski D. A., Frankel R. B. (1998) Iron sulfides from magnetotactic bacteria: structure, composition, and phase transitions. *Am. Mineral.* **83,** 1469–1481.

Pratt A. R., Blowes D. W., Ptacek C. J. (1997) Products of chromate reduction on proposed subsurface remediation material. *Env. Sci. Tech.* **31,** 2492–2498.

Pratt A. R., Nesbitt H. W., Muir I. J. (1994a) X-ray photoelectron and Auger spectroscopic studies of pyrrhotite and mechanism of air oxidation. *Geochim. Cosmochim. Acta.* **58,** 827–841.

Pratt A. R., Nesbitt H. W., Muir I. J. (1994b) Generation of acids from mine waste: oxidative leaching of pyrrhotite in dilute H_2SO_4 solutions at pH 3.0. *Geochim. Cosmochim. Acta.* **48,** 5147–5159.

Pratt A. R., Nesbitt H. W., Mycroft J. R. (1996) The increased reactivity of pyrrhotite and magnetite phases in sulfide mine tailings. *J. Geochem. Explor.* **56,** 1–11.

Rickard D. T. (1969a) The chemistry of iron sulfide formation at low temperatures. *Stockholm Contrib. Geol.* **26,** 67–95.

Rickard D. T. (1969b) The microbiological formation of iron sulfides. *Stockholm Contrib. Geol.* **26,** 49–66.

Rickard D.T. (1995) Kinetics of FeS precipitation: Part 1. Competing reaction mechanisms. *Geochim. Cosmochim. Acta.* **21,** 4367–4379.

Scofield J. H. (1976) Hartree-Slater subshell photoionization cross sections at 1254 and 1487 eV. *Electron. Spectrosc. Related Phenom.* **8,** 129–137.

Sweeney R. E., Kaplan I. R. (1973) Pyrite framboid formation: laboratory synthesis and marine sediments. *Geology.* **68,** 618–634.

Takeno S., Moh G. H., Wang N. (1982) Dry mackinawite synthesis. *Neues Jahrb. Minerall., Abh.* **144,** 291–342.

Taylor L. A., Finger L. W. (1970) Structural refinement and composition of mackinawite. *Carnegie Institute of Washington Geophysical Laboratory Ann. Report.* **69,** 318–322.

Taylor P., Rummery T. E., Owen D. G. (1979) On the conversion of mackinawite to greigite. *J. Inorg. Nucl. Chem.* **41,** 1683–1687.

Thomas J. E., Jones C. F., Skinner W. M., Smart R. St. C. (1998) The role of surface species in the inhibition of pyrrhotite dissolution in acid conditions. *Geochim. Cosmochim. Acta.* **62,** 9., 1555–1565.

Vaughan D. J. (1970) Nickelian mackinawite from Vlakfontein: A reply. *Am. Mineral.* **55,** 1807–1808.

Vaughan D. J., Craig J. R. (1978) Mineral chemistry of metal sulphides. Cambridge Univ. Press, Cambridge. U.K.

Vaughan D. J., Ridout M. S. (1971) Mössbauer studies of some sulfide minerals. *J. Inorg. Nucl. Chem.* **33,** 741–746.

Yamaguchi S., Moori T. (1972) Electrochemical synthesis of ferromagnetic Fe_3S_4. *J. Electrochem. Soc.* **119,** 1062.